Downregulation of *WDR20* due to loss of 14q is involved in the malignant transformation of clear cell renal cell carcinoma

Mika Takahashi,[1,2] Yoshiyuki Tsukamoto,[1] Tomoki Kai,[1,2] Akinori Tokunaga,[3] Chisato Nakada,[1] Naoki Hijiya,[1] Tomohisa Uchida,[1] Tsutomu Daa,[4] Takeo Nomura,[2] Fuminori Sato,[2] Hiromitsu Mimata,[2] Keiko Matsuura[1,5] and Masatsugu Moriyama[1]

Departments of [1]Molecular Pathology; [2]Urology; [3]Research Promotion Institute; [4]Department of Diagnostic Pathology; [5]Department of Biology, Faculty of Medicine, Oita University, Oita, Japan

Previously, we reported that genomic loss of 14q occurs more frequently in high-grade than in low-grade clear cell renal cell carcinomas (ccRCCs), and has a significant impact on the levels of expression of genes located in this region, suggesting that such genes may be involved in the malignant transformation of ccRCCs. Here, we found that six of the genes located in the minimal common region of 14q loss were significantly downregulated in high-grade ccRCCs due to copy number loss. Using a dataset from The Cancer Genome Atlas Research Network, we found that downregulation of one of these six genes, *WDR20*, was significantly associated with poorer outcome in patients with ccRCC, suggesting that WDR20 downregulation may be involved in the malignant transformation of ccRCCs. In functional assays, exogenous WDR20 significantly inhibited the growth of RCC cell lines and induced apoptosis. Interestingly, the phosphorylation levels of ERK and protein kinase B∕AKT, which reportedly contribute to the malignant phenotype of RCC cells, were clearly reduced by exogenous expression of WDR20. Thus, our data suggest that downregulation of WDR20 due to 14q loss may be involved in the malignant transformation of ccRCCs, in part through activation of the ERK and protein kinase B∕AKT pathways.

Renal cell carcinoma (RCC) accounts for approximately 3% of all adult malignancies and 90–95% of all kidney neoplasms.[1] Clear cell RCC (ccRCC) is the most common histological subtype, accounting for approximately 70–80% of RCC cases.[1,2] Among the various clinicopathological features of ccRCC, nuclear grading, also known as the Fuhrman grading,[3] is the most useful prognostic parameter. Patients with nuclear grades 3 and 4 (high-grade) ccRCC have been reported to show a poorer survival rate than those with nuclear grades 1 and 2 (low-grade) ccRCC.[3]

Previously, to reveal the alterations associated with the malignant transformation of ccRCC, we analyzed the genomic alterations in 26 cases of ccRCC (11 low-grade and 15 high-grade). We found that 14q loss occurred more frequently in high-grade than in low-grade ccRCCs, and that many of the genes located on 14q were downregulated due to copy number loss.[4] Recently, using a relatively large cohort (246 cases), Klatte *et al.*[5] also showed that 14q loss was associated with a higher TNM stage, higher nuclear grade, larger tumor size, and poorer prognosis. It has also been reported that 14q loss is associated with poorer survival,[5–8] a higher Fuhrman grading[5,6] and distant metastasis.[5] These data from our group and others[5–8] suggest that 14q loss is involved in the malignant transformation of ccRCC through downregulation of tumor suppressor genes located in this region. However, the mechanism by which 14q loss affects the malignant transformation of ccRCC remains largely unknown.

In the present study, to identify the gene(s) responsible for 14q loss from among those located in the minimal common region involved, 14q32.31-33, determined in our previous study,[4] we compared the expression of these genes between low- and high-grade ccRCCs and analyzed the effect of downregulation of the candidate genes on prognosis by using the ccRCC dataset from The Cancer Genome Atlas (TCGA). Furthermore, we examined the possible tumor-suppressive function of WDR20, whose expression was downregulated in high-grade ccRCC due to copy number loss at14q and associated with poorer prognosis.

Materials and Methods

Details of array data analysis, vector construction, establishment of stable cell lines, removal of integrated cDNA, isolation of cells by cell sorting, RNA extraction, quantitative RT-PCR, invasion assay, gene expression microarray analysis, treatment of cells with 5-aza-2′-deoxycytidine and trichostatin A, and migration assay are provided in Document S1.

Original Article
Downregulation of WDR20 in ccRCC
www.wileyonlinelibrary.com/journal/cas

Patients. Primary tumors of RCC were surgically resected at Oita University Hospital and Oita Red Cross Hospital (Oita, Japan) and diagnosed histopathologically as described previously[4,9] (Table S1). Use of the tissue samples for all experiments was approved by the Oita University Ethics Committee (approval no. P-05-05).

Dataset analysis. Datasets pertaining to mRNA expression, DNA copy number, and clinical information for 499 ccRCC patients from the TCGA Research Network (http://cancergenome.nih.gov/) were analyzed using cBioPortal for Cancer Genomics (http://www.cbioportal.org).[10,11] The patients were considered to have high and low expression of each candidate gene based on Z scores of >0 and <−2, respectively. Also, the genomic copy number status of each candidate gene was determined using Affymetrix (Santa Clara, CA, USA) SNP6 array-based GISTIC analysis, in which values of −2, −1, 0, 1, and 2 represent putative homozygous deletion, hemizygous deletion, no change, gain, and high-level amplification, respectively.

Cell lines. The RCC cell lines 786-O and 769-P were purchased from ATCC (Manassas, VA, USA) and maintained in accordance with the supplier's instructions.

Western blot analysis. Western blotting was carried out as described previously with slight modifications.[12] The primary antibodies were: anti-FLAG M2 (Sigma-Aldrich, St. Louis, MO, USA), anti-p-AKT S473 D9E, anti-pan AKT, anti-p-ERK, anti-total ERK (Cell Signaling Technology, Danvers,

MA, USA), anti-WDR20 (Bethyl, Montgomery, TX, USA), and anti-GAPDH (Sigma-Aldrich). Detection was carried out with ECL Prime Western Blotting Detection Reagents (Amersham Biosciences, Piscataway, NJ, USA) in accordance with the manufacturer's instructions. GAPDH was used as an internal control.

Proliferation assay. We cultured 1×10^3 cells of each cell line in 96-well plates for 0, 48, 72, and 96 h, and measured the viabilities of the cells using the CellTiter96 aqueous one solution cell proliferation assay (Promega, Madison, WI, USA) in accordance with the manufacturer's instructions.

Colony formation assay. For stably transfected cell lines, 100 cells were cultured in 10-cm dishes for 14 days. For transiently transfected cells, 1×10^5 cells were cultured in a 10-cm dish and selected with G418 (1.2 mg/mL) for 14 days. The resulting colonies were fixed with 10% buffered formalin, stained with 0.05% toluidine blue solution (pH 7.0) (Wako, Osaka, Japan) and quantified.

Apoptosis assay. We evaluated the induction of apoptosis by measuring cytoplasmic oligonucleosomal fragments and caspase 3/caspase 7 activities. Cytoplasmic oligonucleosomal fragments of the cells cultured for 72 h in a 96-well plate were measured with a Cell Death Detection ELISA^{PLUS} kit (Roche Applied Science, Mannheim, Germany) in accordance with the manufacturer's instructions. Activities of caspase 3 and 7 in the cells cultured for 96 h in a 96-well plate were determined
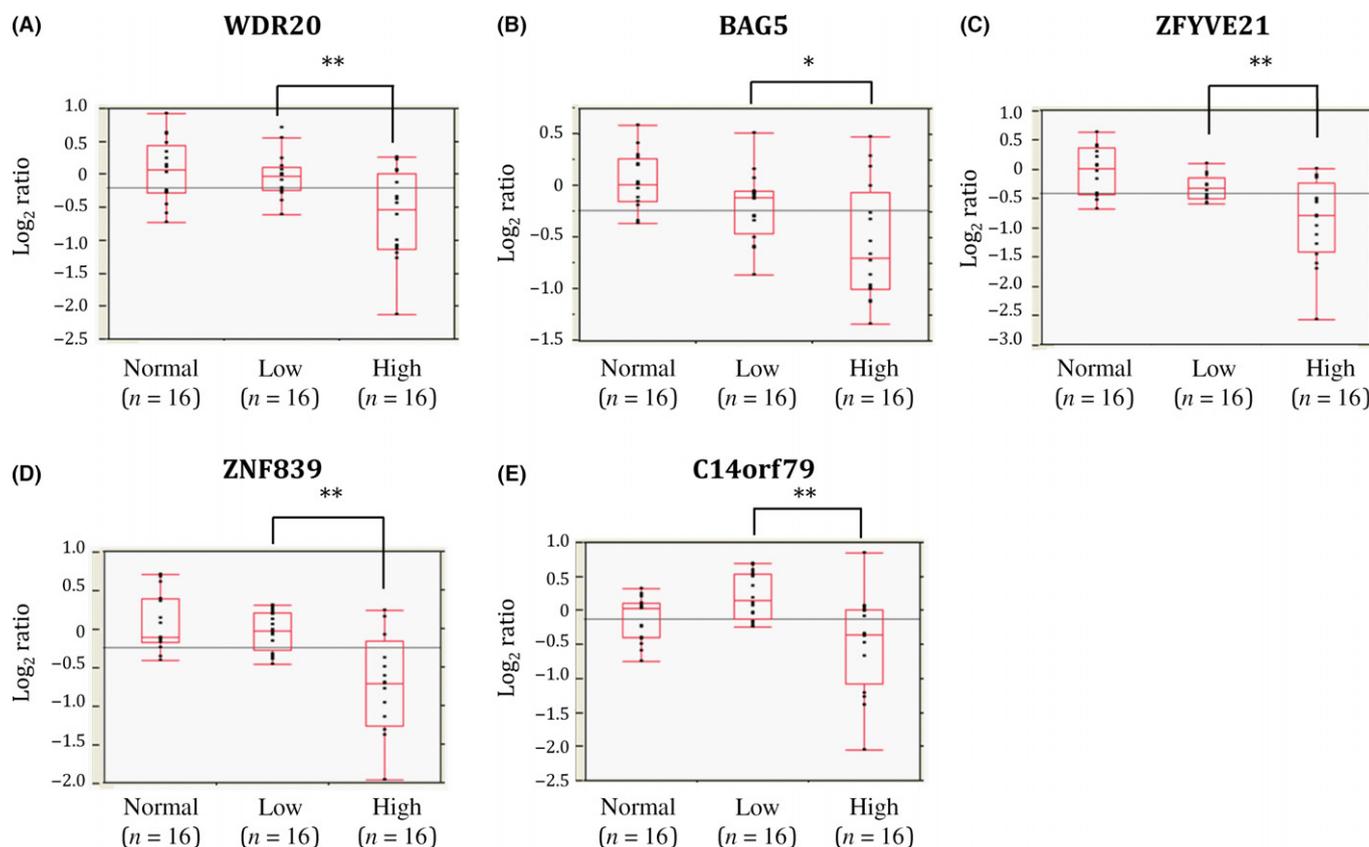

Fig. 1. Significant associations between downregulation of *WDR20*, *BAG5*, *ZFYVE21*, *ZNF839*, and *C14orf79* and high grade in clear cell renal cell carcinomas. Expression levels of *WDR20* (A), *BAG5* (B), *ZFYVE21* (C), *ZNF839* (D), and *C14orf79* (E) were determined by microarray analysis and compared between normal kidney tissues (normal, *n* = 16), and low-grade (low, *n* = 16) and high-grade (high, *n* = 16) clear cell renal cell carcinomas. The *y*-axis represents the expression level (log$_2$) normalized by the median expression level for the 16 normal samples. Comparisons between groups were determined by Wilcoxon test and Tukey–Kramer test. *P < 0.05, **P < 0.01.

using a caspase-Glo 3/7 assay kit (Promega) in accordance with the manufacturer's instructions.

Statistical analysis. Differences in the expression levels of the candidate genes between low- and high-grade ccRCCs were determined by the Wilcoxon test and Tukey–Kramer test. Associations between the expression levels of candidate genes and patient survival were expressed by Kaplan–Meier curves and analyzed by log–rank test in cBioPortal. Differences in quantitative RT-PCR, proliferation, colony formation, invasion, migration, and apoptosis assays were analyzed by two-sided Student's t-test. Values are expressed as mean $\pm$ SEM. Differences at P values of <0.05 were considered to be statistically significant.

Results

Genomic loss of 14q is associated with downregulation of *WDR20*, *BAG5*, *ZFYVE21*, *ZNF839*, and *C14orf79* in high-grade ccRCCs. To identify genes located in the minimal common region of 14q loss and downregulated due to copy number loss, we compared the gene expression profiles of ccRCCs with and without 14q loss. Among the genes located on 14q32.31-33, six showed an expression level of <0.75 in cases with 14q loss relative to those without 14q loss (Table S2). In addition, we found that five of these six genes were significantly downregulated in high-grade relative to low-grade ccRCCs while the remaining gene showed no difference, suggesting that downregulation of these five genes, *WDR20*, *BAG5*, *ZFYVE21*, *ZNF839*, and *C14orf79*, may be related to malignant transformation of ccRCC (Table S2, Figs 1, S1).

Downregulation of *WDR20* due to copy number loss is related to poorer outcome of patients with ccRCCs. Next, we analyzed the associations between downregulation of each of the above

five genes and patient survival using a TCGA dataset.[13] Although downregulation of four of the five genes had no correlation with prognosis, a lower level of WDR20 expression was significantly associated with a poorer outcome (Figs 2A, S2). As shown in Figure 2(B), we also found that patients with *WDR20* gene copy number loss showed a poorer outcome than those without such loss. Furthermore, the copy number of *WDR20* was strongly correlated with the level of its mRNA (Fig. 2C). These results suggest that downregulation of *WDR20* due to genomic copy number loss is associated with poorer survival of patients with ccRCCs. The expression level and copy number of *WDR20* were also significantly associated with T stage, lymph node metastasis, and distant metastasis in the TCGA dataset (Table S3). A significant association between *WDR20* expression and T stage was also observed in our dataset (Fig. S3). Additionally, our dataset revealed a tendency for an association between *WDR20* expression and vascular involvement, although this did not reach statistical significance ($P = 0.0975$, Fig. S3).

Although almost all ccRCCs with 14q loss showed single-copy genomic loss of *WDR20* as judged by array CGH analysis,[4] mutational inactivation of the remaining *WDR20* allele appeared unlikely, as somatic mutation of *WDR20* was not detected at all in the TCGA dataset. However, treatment with a combination of the DNA demethylating agent 5-aza-dC and the histone deacetylase inhibitor trichostatin A (TSA) resulted in slight but statistically significant upregulation of *WDR20* (Fig. S4), suggesting that epigenetic modifications may be partly involved in silencing of *WDR20* on the remaining allele in ccRCC with 14q loss (Fig. S4).

Exogenous expression of WDR20 inhibits cell proliferation and induces apoptosis in RCC cells. To determine whether expression of *WDR20* regulates the proliferation of RCC cells, we trans-
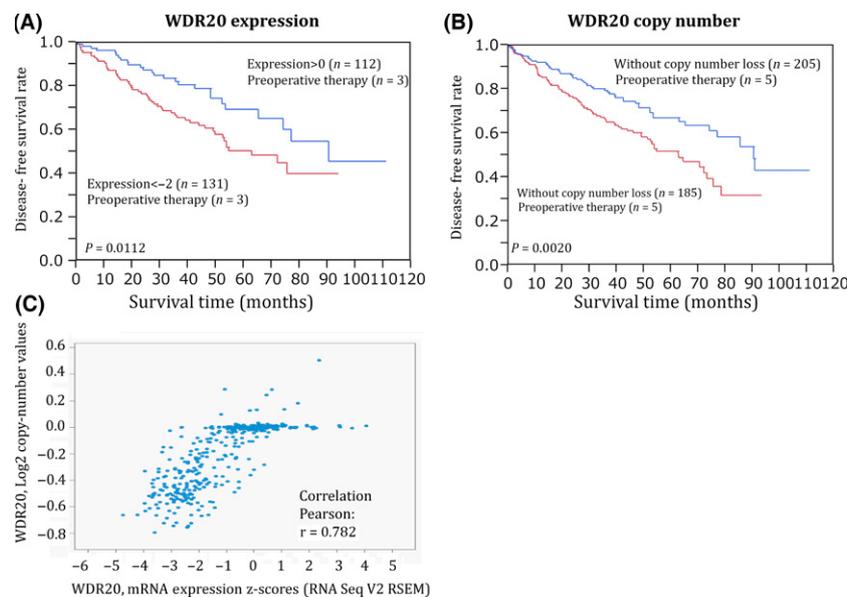

Fig. 2. Correlation between mRNA level or copy number of *WDR20* and disease-free survival rate in patients with clear cell renal cell carcinoma (ccRCC). Kaplan–Meier survival curves of the disease-free survival rate in patients with ccRCCs according to the expression level (A) and copy number status (B) of *WDR20* were generated using The Cancer Genome Atlas dataset. (A) Patients with low *WDR20* expression (Z score <−2, $n = 131$; preoperative therapy, $n = 3$) had a significantly worse survival rate than those with high *WDR20* expression (Z score >0, $n = 112$; preoperative therapy, $n = 3$) as determined by log–rank test ($P = 0.0112$). (B) Patients with genomic copy number loss of *WDR20* from GISTIC analysis (GISTIC $\leq$−1, $n = 185$; preoperative therapy, $n = 5$) had a significantly worse survival rate than those without loss of *WDR20* (GISTIC $\geq$0, $n = 205$; preoperative therapy, $n = 5$) as determined by log–rank test ($P = 0.002$). (C) The genomic copy number of *WDR20* was significantly correlated with the expression level of *WDR20* in 394 cases of ccRCC obtained from The Cancer Genome Atlas dataset (Pearson correlation coefficient = 0.782, $P < 0.01$)
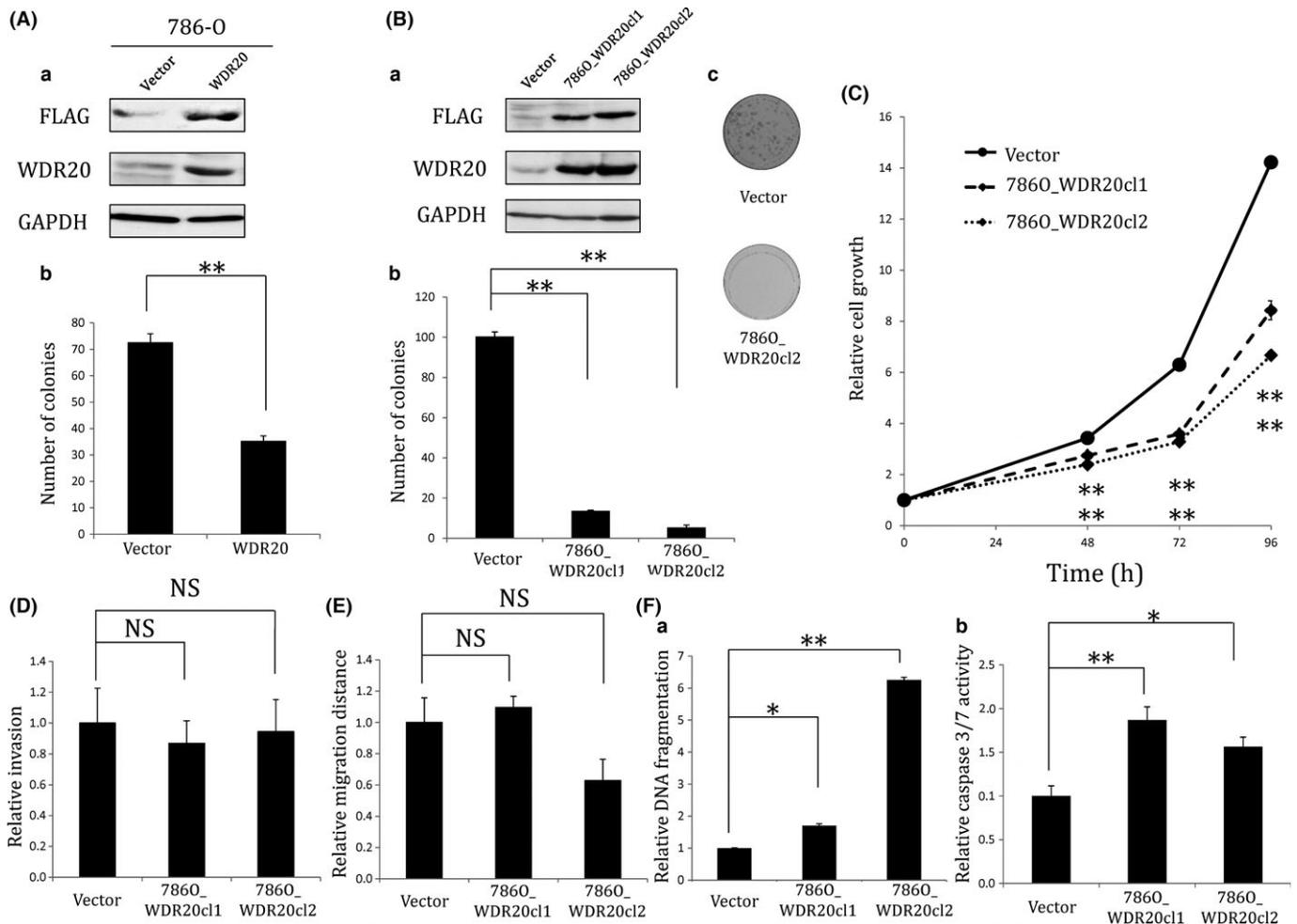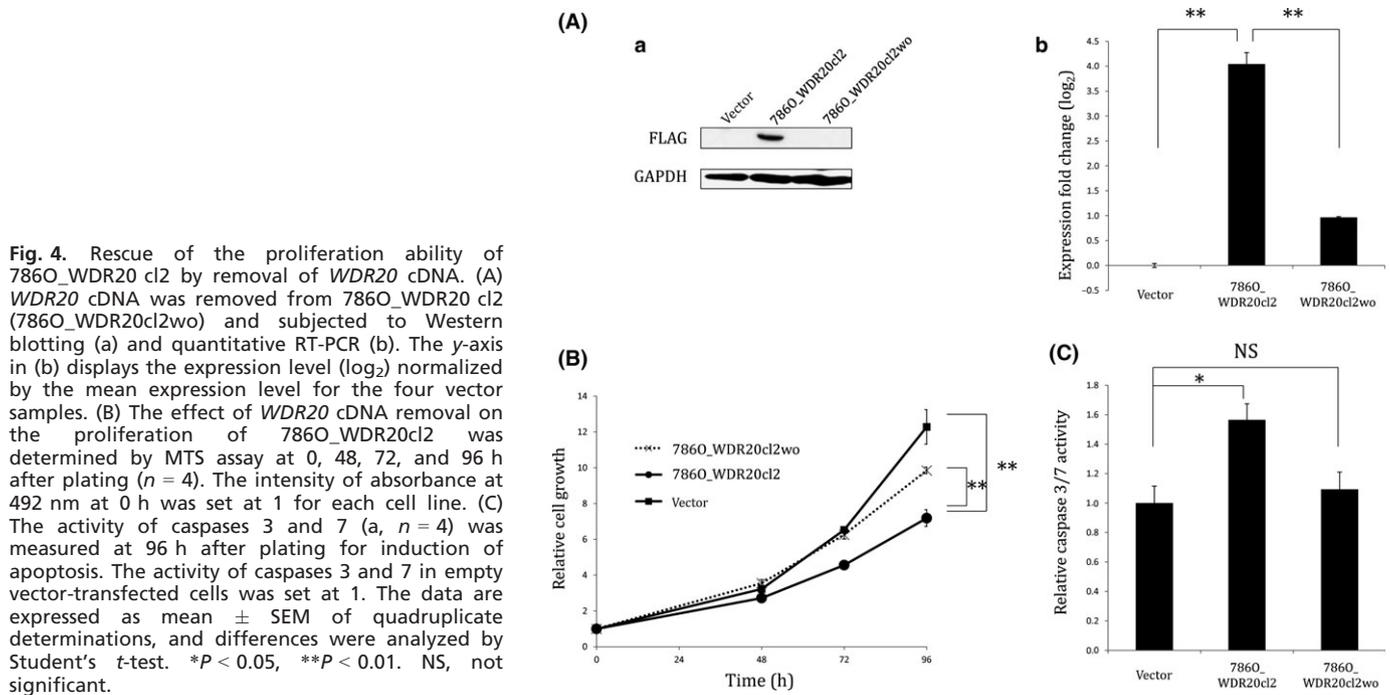
Original Article
Downregulation of WDR20 in ccRCC
www.wileyonlinelibrary.com/journal/cas

Fig. 3. Ectopic expression of *WDR20* suppresses cell proliferation and induces apoptosis in renal cell carcinoma cells. (A) 786-O cells were transiently transfected with WDR20-pPB-Ubc-FLIG and subjected to Western blotting (a) and colony formation assay (b, $n = 3$). (B) 786-O cells were stably transfected with WDR20-pPB-Ubc-FLIG and subjected to Western blotting (a) and colony formation assay (b, $n = 3$). Representative images of the resulting colonies are shown in (c). (C) Viabilities of stably transfected cell lines were determined by MTS assay at 0, 48, 72, and 96 h after plating ($n = 4$). The intensity of absorbance at 492 nm at 0 h was set at 1 for each cell line. (D) Invasiveness of stably transfected cell lines was determined by Matrigel invasion assay ($n = 4$). The fluorescence intensity at 494/517 nm of empty vector-transfected cells was set at 1. (E) Migration ability was determined using Oris Cell Migration Assay – Collagen I-coated 96-well plates ($n = 4$). The migration distance of empty vector-transfected cells was set at 1. (F) Cytoplasmic oligonucleosomal fragment (a, $n = 4$), and activities of caspases 3 and 7 (b, $n = 4$) were measured for evaluation of apoptosis. The value for empty vector-transfected cells was set at 1. The data are expressed as mean ± SEM of quadruplicate determinations, and differences were analyzed by Student's *t*-test. *$P < 0.05$, **$P < 0.01$. NS, not significant.

fected 786-O cells, which show hemizygous loss and downregulation of *WDR20*[14](Fig. S5), with a plasmid encoding FLAG-tagged *WDR20* cDNA and carried out colony formation assays. Overexpression of *WDR20* in the transfected cells was confirmed by Western blotting (Fig. 3Aa). As shown in Figure 3(Ab), exogenous *WDR20* significantly inhibited the colony-forming ability of 786-O. Next, we established two 786-O cell lines, 786O_WDR20 cl1 and 786O_WDR20 cl2, stably expressing *WDR20* (Figs 3Ba,S6), and carried out colony formation assays. Both cell lines formed fewer colonies and showed a slower growth rate than control cells (Figs 3Bb,c,C). The growth-suppressive function of WDR20 was confirmed by using another RCC cell line, 769-P, showing hemizygous loss and downregulation of *WDR20*[14](Fig. S5). We established two cell lines, 769P_WDR20 cl1 and 769P_ WDR20 cl2, stably expressing *WDR20* in 769-P. Despite only a slight increase in the level of *WDR20* mRNA in the established cells (Fig. S7A), their growth was suppressed, as assessed by MTS

assay (Fig. S7B). We noticed that significant inhibition of cell viability by *WDR20* took longer to appear in 769-P than in 786-O cells. This may have been due to the difference in the growth speed and level of ectopically expressed *WDR20* between the two cell lines. We also investigated the effect of *WDR20* expression on RCC cell invasiveness, motility, and apoptosis. Overexpression of *WDR20* had little effect on the invasiveness and motility of 786-O cells (Fig. 3D,E), but significantly induced apoptosis as assessed by detection of cytoplasmic oligonucleosomal fragments or activated caspase 3/7 (Fig. 3F). Taken together, our results suggest that expression of *WDR20* inhibits the growth of RCC cells partly through induction of apoptosis.

To confirm the growth-suppressive and apoptosis-inducing effect of *WDR20*, we removed cDNA of *WDR20* from its stable transfectant, 786O_WDR20 cl2, using transposase, and established a subclone, 786O_WDR20 cl2wo, in which expression of *WDR20* was substantially decreased at both the protein

Fig. 4. Rescue of the proliferation ability of 786O_WDR20 cl2 by removal of WDR20 cDNA. (A) WDR20 cDNA was removed from 786O_WDR20 cl2 (786O_WDR20cl2wo) and subjected to Western blotting (a) and quantitative RT-PCR (b). The y-axis in (b) displays the expression level ($\log_2$) normalized by the mean expression level for the four vector samples. (B) The effect of WDR20 cDNA removal on the proliferation of 786O_WDR20cl2 was determined by MTS assay at 0, 48, 72, and 96 h after plating ($n = 4$). The intensity of absorbance at 492 nm at 0 h was set at 1 for each cell line. (C) The activity of caspases 3 and 7 (a, $n = 4$) was measured at 96 h after plating for induction of apoptosis. The activity of caspases 3 and 7 in empty vector-transfected cells was set at 1. The data are expressed as mean ± SEM of quadruplicate determinations, and differences were analyzed by Student's t-test. *$P < 0.05$, **$P < 0.01$. NS, not significant.
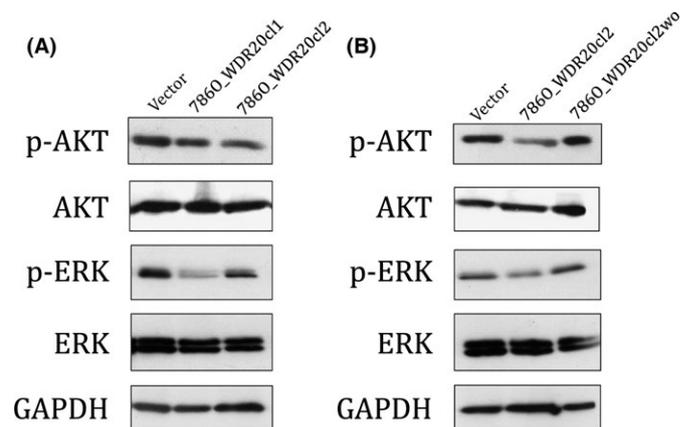
and mRNA levels (Fig. 4A). As shown in Figure 4(B,C), we found that the growth rate inhibition and apoptosis induction in 786O_WDR20 cl2 were reduced to almost the same levels as those in the parental 786-O cells by removal of WDR20 cDNA, confirming that the growth inhibition and apoptosis induction in 786O_ WDR20 cl2 were caused by the ectopically expressed WDR20.

Expression of WDR20 suppresses phosphorylation levels of AKT and ERK. To determine the mechanism by which WDR20 inhibits cell growth and induces apoptosis, we analyzed the effect of WDR20 overexpression on the activities of the RAF/MEK/ERK and PI3K/AKT/MTOR pathways using Western blotting. As shown in Figure 5, exogenous WDR20 suppressed the phosphorylation of both ERK and AKT, whereas removal of WDR20 cDNA reduced this suppression to the same level as that in the parental cells, suggesting that the level of WDR20 expression is associated with activation of both ERK and AKT. We also found that several of the genes related to the RAF/MEK/ERK and/or PI3K/AKT/MTOR pathways were differentially expressed by the ectopic expression of WDR20 (Table S4). Therefore, we concluded that growth inhibition and apoptosis induction by WDR20 are due, at least partly, to suppression of the ERK and AKT pathways.

Fig. 5. WDR20 suppresses the phosphorylation of protein kinase B (AKT) and ERK in renal cell carcinoma cells. At 72 h after plating, the vector, 786O_WDR20 cl1, and 786O_WDR20 cl2 (A) or the vector, 786O_WDR20 cl2, and 786O_WDR20cl2wo (B) were subjected to Western blot analysis using antibodies against the phosphorylated form of AKT (Ser473), total AKT, the phosphorylated form of ERK (Thr202/Tyr204), total ERK, and GAPDH.

Discussion

To identify genes whose downregulation affects the malignant characteristics of ccRCC, we focused on the minimal common region of 14q loss, which we had defined previously as 14q32.31-33.[4] Among the genes located in the minimal common region, WDR20, BAG5, ZFYVE21, ZNF839, and C14orf79 were significantly downregulated in high-grade ccRCC due to copy number loss. Although upregulation of BAG5 and ZFYVE21 is reportedly associated with apoptosis resistance in prostate cancer[15] and metastasis of colorectal carcinoma,[16] respectively, it has not yet been determined whether downregulation of any of these genes is related to tumor malignancy. In the present study, we showed for the first time that a lower level of WDR20 expression was signifi-

cantly associated with poorer outcome in patients with ccRCC. Although we cannot exclude the possibility that the other five genes also have tumor-suppressive roles in ccRCC, our data suggest that downregulation of WDR20 due to 14q loss contributes to the malignant transformation of ccRCC.

In this study, we found that overexpression of WDR20 induced growth suppression and apoptosis in ccRCC cells. WDR20 is a member of the WD (tryptophan–aspartate) repeat family of proteins that have four to 16 WD domains, each of which possesses a conserved core sequence comprising approximately 40 amino acids flanked by a GH (glycine–histidine) dipeptide at the N-terminus and a WD dipeptide at the C-terminus.[17] It has been reported that WDR20, which has five WD domains, is a component of the deubiquitinase complex and

stimulates the activities of two deubiquitinating enzymes, ubiquitin-specific peptidase (USP)12 USP46, cooperatively with USP1-associated factor 1 (UAF1).[18] Although there are no reports about the tumor-suppressive role of WDR20, the involvement of USP12 and USP46 in tumorigenesis has been reported previously. USP12 is known to deubiquitinate histones H2B and H2A and induce apoptosis when overexpressed in prostate cancer cells.[19] USP12 has also been reported to inhibit the growth of prostate cancer cells by deubiquitinating PHLPP1 that dephosphorylates and inactivates AKT.[20,21] In addition, in colon cancer, it has been reported that USP46 plays a role in inhibiting the activation of AKT through deubiquitination of PHLPP1 in coordination with WDR20 and USP1-associated factor 1.[22] Therefore, together with these previous reports, our data suggest that *WDR20* might exert its tumor-suppressive function through regulation of deubiquitinating enzymes, such as USP12 and USP46. Further studies are required to clarify the mechanism whereby *WDR20* induces growth suppression and apoptosis in ccRCC cells.

In the present study, we found that overexpression of *WDR20* suppressed the phosphorylation of AKT and ERK. Aberrant activation of the PI3K/AKT/MTOR and RAF/MEK/ERK pathways is frequently observed in various types of cancer, including ccRCC, and enhances the proliferation or survival of cancer cells.[13,23,24] In ccRCC, enhanced activation of the PI3K/AKT/MTOR pathway is frequently observed, and this is correlated with local invasion, regional lymph node involvement, microscopic vascular invasion, distant metastasis, and poor prognosis.[25,26] At the same time, it has been reported that a high level of phospho-ERK is frequently observed in ccRCC and correlated with poor prognosis, tumor size, invasiveness, and clinical stage.[23,27] Interestingly, molecular targeted agents that block aberrant activation of the PI3K

/AKT/MTOR and/or RAF/MEK/ERK pathways, such as MTOR and multiple receptor tyrosine kinase inhibitors, are currently used for first-line treatment of ccRCC, suggesting that activation of these pathways is the driver of ccRCC.[28–30] Thus, our data suggest that *WDR20* suppresses the growth of ccRCC cells, at least partly, through inhibition of these driver pathways. Further studies to clarify the mechanism whereby *WDR20* regulates the phosphorylation of AKT and ERK might provide a much better understanding of feasible therapeutic strategies for ccRCC.

Disclosure Statement

The authors have no conflict of interest.

Abbreviations

AKT	protein kinase B
ccRCC	clear cell renal cell carcinoma
mTOR	mammalian target of rapamycin
PHLPP1	PH domain and leucine-rich repeat protein phosphatase 1
PI3K	phosphatidylinositol 3-kinase
RCC	renal cell carcinoma
TCGA	The Cancer Genome Atlas
UAF1	ubiquitin-specific peptidase 1-associated factor 1
USP	ubiquitin-specific peptidase

References

1 Corgna E, Betti M, Gatta G, Roila F, De Mulder PH. Renal cancer. *Crit Rev Oncol Hematol* 2007; **64**: 247–62.

2 Reuter VE. The pathology of renal epithelial neoplasms. *Semin Oncol* 2006; **33**: 534–43.

3 Fuhrman SA, Lasky LC, Limas C. Prognostic significance of morphologic parameters in renal cell carcinoma. *Am J Surg Pathol* 1982; **6**: 655–63.

4 Yoshimoto T, Matsuura K, Karnan S *et al.* High-resolution analysis of DNA copy number alterations and gene expression in renal clear cell carcinoma. *J Pathol* 2007; **213**: 392–401.

5 Klatte T, Rao PN, de Martino M *et al.* Cytogenetic profile predicts prognosis of patients with clear cell renal cell carcinoma. *J Clin Oncol* 2009; **27**: 746–53.

6 Alimov A, Sundelin B, Wang N, Larsson C, Bergerheim U. Loss of 14q31-q32.2 in renal cell carcinoma is associated with high malignancy grade and poor survival. *Int J Oncol* 2004; **25**: 179–85.

7 Arai E, Kanai Y. Genetic and epigenetic alterations during renal carcinogenesis. *Int J Clin Exp Pathol* 2010; **4**: 58–73.

8 Shuib S, Wei W, Sur H *et al.* Copy number profiling in von Hippel-Lindau disease renal cell carcinoma. *Genes Chromosom Cancer* 2011; **50**: 479–88.

9 Narimatsu T, Matsuura K, Nakada C *et al.* Downregulation of NDUFB6 due to 9p24.1-p13.3 loss is implicated in metastatic clear cell renal cell carcinoma. *Cancer med* 2015; **4**: 112–24.

10 Gao J, Aksoy BA, Dogrusoz U *et al.* Integrative analysis of complex cancer genomics and clinical profiles using the cBioPortal. *Sci Signal* 2013; **6**: pl1.

11 Cerami E, Gao J, Dogrusoz U *et al.* The cBio cancer genomics portal: an open platform for exploring multidimensional cancer genomics data. *Cancer Discov* 2012; **2**: 401–4.

12 Shomori K, Nagashima Y, Kuroda N *et al.* ARPP protein is selectively expressed in renal oncocytoma, but rarely in renal cell carcinomas. *Mod Pathol* 2007; **20**: 199–207.

13 Comprehensive molecular characterization of clear cell renal cell carcinoma. *Nature* 2013;**499**:43–9.

14 Matsuura K, Nakada C, Mashio M *et al.* Downregulation of SAV1 plays a role in pathogenesis of high-grade clear cell renal cell carcinoma. *BMC Cancer* 2011; **11**: 523.

15 Bruchmann A, Roller C, Walther TV *et al.* Bcl-2 associated athanogene 5 (Bag5) is overexpressed in prostate cancer and inhibits ER-stress induced apoptosis. *BMC Cancer* 2013; **13**: 96.

16 Nagano M, Hoshino D, Koshiba S *et al.* ZF21 protein, a regulator of the disassembly of focal adhesions and cancer metastasis, contains a novel noncanonical pleckstrin homology domain. *J Bio Chem* 2011; **286**: 31598–609.

17 Smith TF, Gaitatzes C, Saxena K, Neer EJ. The WD repeat: a common architecture for diverse functions. *Trends Biochem Sci* 1999; **24**: 181–5.

18 Kee Y, Yang K, Cohn MA, Haas W, Gygi SP, D'Andrea AD. WDR20 regulates activity of the USP12 x UAF1 deubiquitinating enzyme complex. *J Bio Chem* 2010; **285**: 11252–7.

19 Burska UL, Harle VJ, Coffey K *et al.* Deubiquitinating enzyme Usp12 is a novel co-activator of the androgen receptor. *J Bio Chem* 2013; **288**: 32641–50.

20 McClurg UL, Summerscales EE, Harle VJ, Gaughan L, Robson CN. Deubiquitinating enzyme Usp12 regulates the interaction between the androgen receptor and the Akt pathway. *Oncotarget* 2014; **5**: 7081–92.

21 Gangula NR, Maddika S. WD repeat protein WDR48 in complex with deubiquitinase USP12 suppresses Akt-dependent cell survival signaling by stabilizing PH domain leucine-rich repeat protein phosphatase 1 (PHLPP1). *J Bio Chem* 2013; **288**: 34545–54.

22 Li X, Stevens PD, Yang H *et al.* The deubiquitination enzyme USP46 functions as a tumor suppressor by controlling PHLPP-dependent attenuation of Akt signaling in colon cancer. *Oncogene* 2013; **32**: 471–8.

23 Li XL, Chen XQ, Zhang MN *et al.* SOX9 was involved in TKIs resistance in renal cell carcinoma via Raf/MEK/ERK signaling pathway. *Int J Clin Exp Pathol* 2015; **8**: 3871–81.

24 Husseinzadeh HD, Garcia JA. Therapeutic rationale for mTOR inhibition in advanced renal cell carcinoma. *Curr Clin Pharmacol* 2011; **6**: 214–21.

25 Mizuno T, Kamai T, Abe H *et al.* Clinically significant association between the maximum standardized uptake value on (1)(8)F-FDG PET and expres-

sion of phosphorylated Akt and S6 kinase for prediction of the biological characteristics of renal cell cancer. *BMC Cancer* 2015; **15**: 114.
26 Campbell L, Jasani B, Edwards K, Gumbleton M, Griffiths DF. Combined expression of caveolin-1 and an activated AKT/mTOR pathway predicts reduced disease-free survival in clinically confined renal cell carcinoma. *Br J Cancer* 2008; **98**: 931–40.
27 Campbell L, Nuttall R, Griffiths D, Gumbleton M. Activated extracellular signal-regulated kinase is an independent prognostic factor in clinically confined renal cell carcinoma. *Cancer* 2009; **115**: 3457–67.

28 Escudier B, Eisen T, Stadler WM *et al.* Sorafenib in advanced clear-cell renal-cell carcinoma. *N Engl J Med* 2007; **356**: 125–34.
29 Bex A, Larkin J, Voss M. Challenging the treatment paradigm for advanced renal cell carcinoma: a review of systemic and localized therapies. *Am Soc Clin Oncol Educ Book* 2015; **35**: e239–47.
30 Fang Z, Tang Y, Fang J *et al.* Simvastatin inhibits renal cancer cell growth and metastasis via AKT/mTOR, ERK and JAK2/STAT3 pathway. *PLoS ONE* 2013; **8**: e62823.

Supporting Information

Additional supporting information may be found in the online version of this article:

Fig. S1. Gene not showing a significant difference in expression level between low- and high-grade clear cell renal cell carcinomas.

Fig. S2. Comparison between mRNA levels for the various genes and disease-free survival rate in patients with clear cell renal cell carcinoma.

Fig. S3. Correlation between *WDR20* expression and T stage and vascular involvement in our own dataset (Table S1).

Fig. S4. Involvement of epigenetic modifications in the downregulation of *WDR20* in 786-O cells.

Fig. S5. Expression of *WDR20* in HEK293T and renal cell carcinoma cell lines.

Fig. S6. Expression levels of WDR20 mRNA in the vector, 786O_WDR20 cl1 and 786O_WDR20 cl2.

Fig. S7. Stable transfection of *WDR20* in 769-P cells.

Fig. S8. Isolation of GFP-negative cells from pCMV-hyPBase-transfected 786O_WDR20 cl2 cells.

Table S1. Clinicopathological information of patients with clear cell renal cell carcinoma

Table S2. Candidate genes significantly downregulated in high-grade clear cell renal cell carcinoma along with 14q loss

Table S3. Correlations between mRNA level or copy number of *WDR20* and pathological features of The Cancer Genome Atlas dataset

Table S4. Upregulated and downregulated molecules in cell lines stably overexpressing *WDR20*, as determined by expression microarray analysis

Doc. S1. Supplementary materials and methods.